

**Search for heavy resonances decaying to a pair of
Higgs bosons in four b quark final state in pp
collisions at $\sqrt{s} = 13$ TeV using the CMS detector at
the LHC**

by

Gregorio de Leon III

Submitted to the Department of Physics
in partial fulfillment of the requirements for the degree of

Master of Science

at the

NATIONAL CENTRAL UNIVERSITY

© National Central University 2017. All rights reserved.

Author

Department of Physics
August 10, 2017

Certified by

Shin-Shan Eiko Yu
Associate Professor
Thesis Supervisor

Accepted by

Professor
Chairman, Thesis Committee

Contents

1	Introduction and Theory Overview	1
1.1	Introduction	1
1.2	Theory	1
2	The LHC and the CMS Detector	3
2.1	Large Hadron Collider	3
2.2	Compact Muon Solenoid	6
2.2.1	Coordinate System	7
2.2.2	Magnet System	9
2.2.3	Inner Tracking System	9
	Pixel Detector	11
	Strip Tracker	12
2.2.4	Electromagnetic Calorimeter	13
2.2.5	Hadron Calorimeter	14
2.2.6	Muon Detector	17
2.3	The Trigger System	17
	Bibliography	19

List of Figures

2.1	Overview of the LHC	4
2.2	The CERN accelerator complex	4
2.3	2015 proton run performance	5
2.4	The CMS detector	7
2.5	CMS coordinate system	8
2.6	CMS tracker system	11
2.7	CMS ECAL system	14
2.8	CMS HCAL system	15

List of Tables

2.1 Parameters of the CMS magnet.	10
---	----



Chapter 1

Introduction and Theory Overview

1.1 Introduction

1.2 Theory



Chapter 2

The LHC and the CMS Detector

The data used in this analysis is collected by the **Compact Muon Solenoid** (CMS) detector at the **Large Hadron Collider** (LHC). The CMS is one of the general-purpose detectors at the LHC which aims to search for extra dimensions, dark matter, and etc [1]. In this chapter, a brief overview of the LHC and the CMS detector is presented.

2.1 Large Hadron Collider

Built by the **European Organization for Nuclear Research** (also known as “CERN”; derived from *Conseil Européen pour la Recherche Nucléaire*) from 1998 to 2008, the LHC is a 27 km in circumference particle collider which lies 175 m beneath the ground of the France-Switzerland border (Figure 2.1). It is the largest and most powerful proton-proton collider in the world. It is also a collaboration of more than 10,000 scientists and engineers coming from different universities and research centers all over the globe [2].

The experiment in the LHC starts with a hydrogen gas that is injected into the source chamber of the **Linear accelerator 2** (LINAC2), in order to remove its electrons. The bunch of protons left is accelerated, with an electric field, in the LINAC2 to reach its energy of 50 MeV. The protons are then fed to the **Proton Synchrotron Booster** (PSB) to accelerate up to 1.4 GeV. After the PSB, it is flung on to the **Proton Synchrotron** (PS) where it is accelerated to 25 GeV. Packets



FIGURE 2.1: Overall view of the LHC (Top view (A) and underground sketch (B)) at the Swiss-French Border from Reference [3].

of protons are then channeled to the **Super Proton Synchrotron** (SPS) which is specifically designed to accept the protons at this energy and further increase it up to 450 GeV. Finally, the SPS launches the protons in the **LHC**. There are two vacuum pipes in the LHC, one circulates the protons clockwise and the other counter-clockwise. A total of 2808 packets of protons is launched by the SPS in the LHC. The LHC adds up the energy of each proton to reach 6.5 TeV [4].

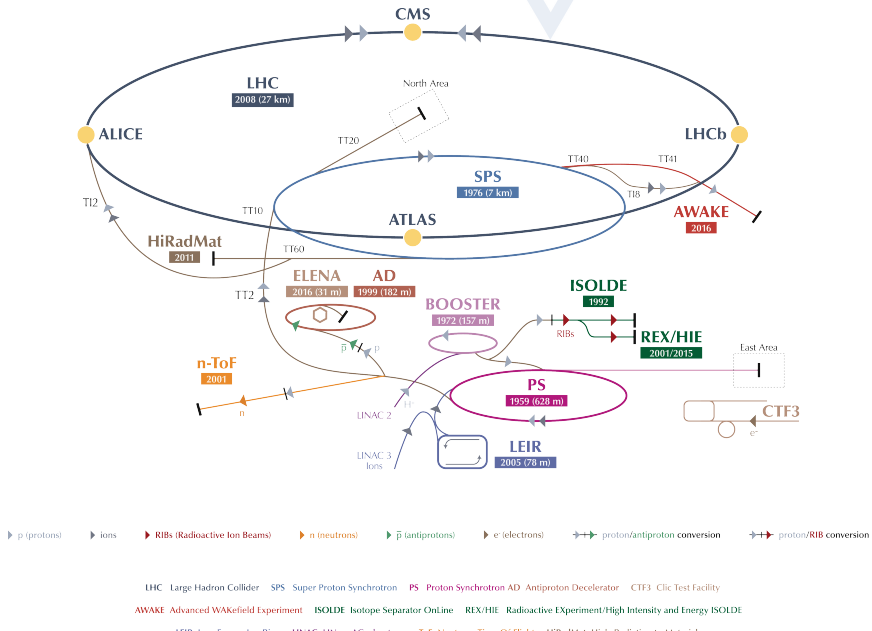


FIGURE 2.2: Schematic view of the CERN accelerator complex. The dark blue circle represents the LHC ring. The smaller machines are used in a chain to help boost the particles to their final energies and provide beams to a whole set of smaller experiments, which also aim to uncover the mysteries of the Universe.

Figure from Reference [5].

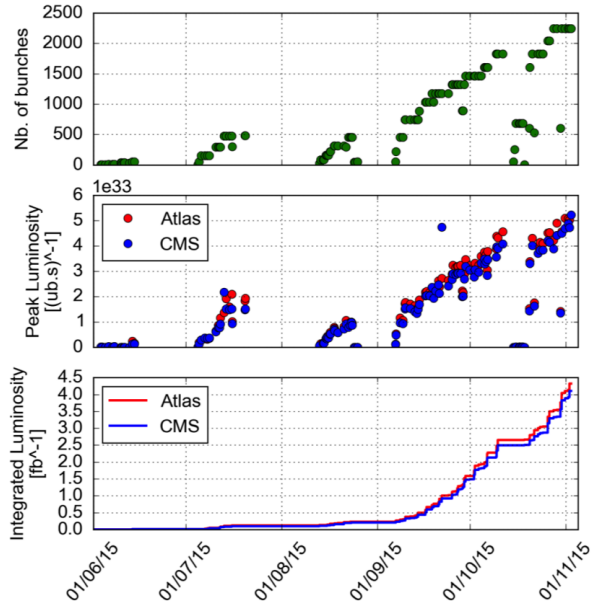


FIGURE 2.3: Progression summary of 2015 proton run performance for the total number of bunches, peak, and integrated luminosities. Figure from Reference [6].

There are four **intersection points** in the LHC, which corresponds to the four main experiments; the “**A Large Ion Collider Experiment**” (ALICE), the “**Large Hadron Collider beauty**” (LHCb), the “**A Toriodial LHC ApparatuS**” (ATLAS), and the **CMS**. ALICE is a heavy-ion (Pb-Pb nuclei) detector that studies the physics of strongly interacting matter at extreme energy densities specifically the quark-gluon plasma, a phase of matter thought to have formed just after the big bang. LHCb uses the particle “beauty quark” or “b quark” to study the differences between matter and antimatter. ATLAS and CMS are the two general-purpose detectors at the LHC with same specific goals, to search for extra dimensions, dark matter, and etc., but both detectors have different scientific solutions and system design [1].

A center-of-mass energy of 13 TeV with 25 ns beam was attained during the Run-II of the LHC in 2015. It was reported that 2244 proton bunches per beam were providing an approximate of $5.0 \times 10^{33} \text{ cm}^{-2}\text{s}^{-1}$ peak luminosities and 4 fb^{-1} total delivered integrated luminosity in both CMS and ATLAS (see Figure 2.3) [6].

2.2 Compact Muon Solenoid

Located approximately 100 m beneath the ground of Cessy, France, the CMS is one of the multi-purpose particle detector operating at the LHC having multi-objectives such as studying SM, including the recently discovered Higgs Boson, and searching for extra dimensions and dark matter particles. Despite having same objectives with the ATLAS detector, it has different scientific solutions and distinct designs such as a high-field solenoid, a full-silicon-based inner tracking system, and a homogenous scintillating-crystals-based electromagnetic calorimeter [1, 7].

CMS satisfies these following detector requirements in order to achieve its objectives [7]:

- Good muon identification and momentum resolution over a wide range of momenta and angles, good dimuon mass resolution ($\approx 1\%$ at 100 GeV), and the ability to determine unambiguously the charge of muons with $p < 1$ TeV;
- Good charged-particle momentum resolution and reconstruction efficiency in the inner tracker. Efficient triggering and offline tagging of τ 's and b -jets, requiring pixel detectors close to the interaction region;
- Good electromagnetic energy resolution, good diphoton and dielectron mass resolution ($\approx 1\%$ at 100 GeV), wide geometric coverage, π^0 rejection, and efficient photon and lepton isolation at high luminosities;
- Good missing-transverse-energy and dijet-mass resolution, requiring hadron calorimeters with a large hermetic geometric coverage and with fine lateral segmentation.

CMS most distinct feature is the 13 m long, 6 m inner-diameter, 3.8 T **superconducting solenoid** (Section 2.2.2) located at the heart of the detector. From

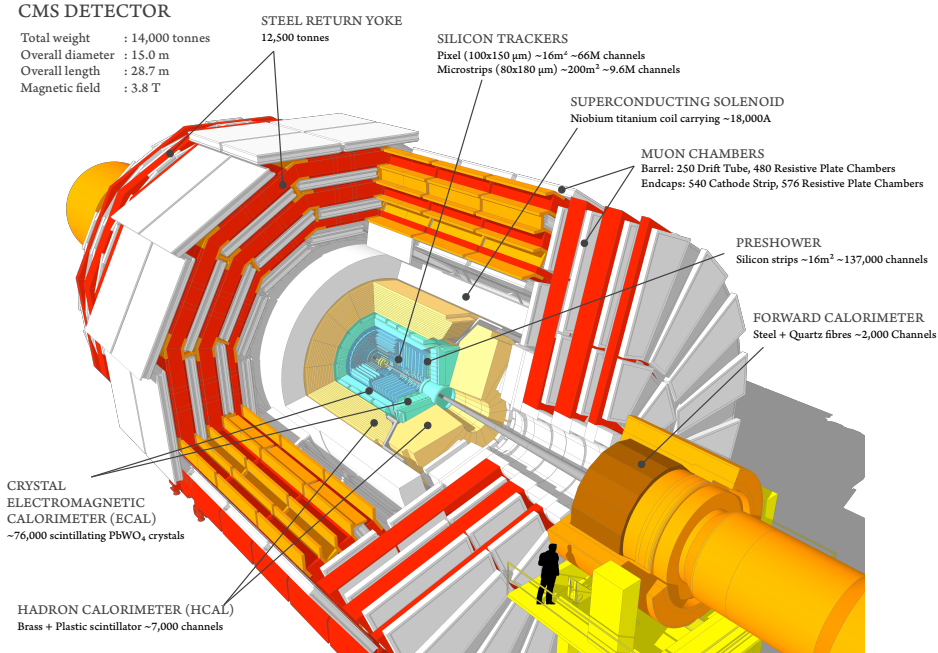


FIGURE 2.4: Cutaway view of the CMS detector from Reference [8].

the inner to the outer layer of the magnet's bore are the **silicon-based tracker** (Section 2.2.3), the **electromagnetic calorimeter** (ECAL) (Section 2.2.4), and the **hadron calorimeter** (HCAL) (Section 2.2.5). Outside of the magnet are the **muon chambers** (Section 2.2.6) [7].

The overall dimension of the CMS detector is 28.7 m long, 15 m diameter, and weighs about 14,000 t [8].

2.2.1 Coordinate System

The origin of the CMS detector's coordinate system is the nominal collision point in the experiment. Its x -axis points towards the center of the LHC ring while its y -axis points vertically upward. Hence, its z -axis points along the beam direction clockwise. In the x - y plane, the radial coordinate is denoted by r and the azimuthal angle (ϕ) is measured from the x -axis (Figure 2.5) [7]. Conventionally, the spherical coordinate system is used due to the detector's axis of symmetry along the z axis.

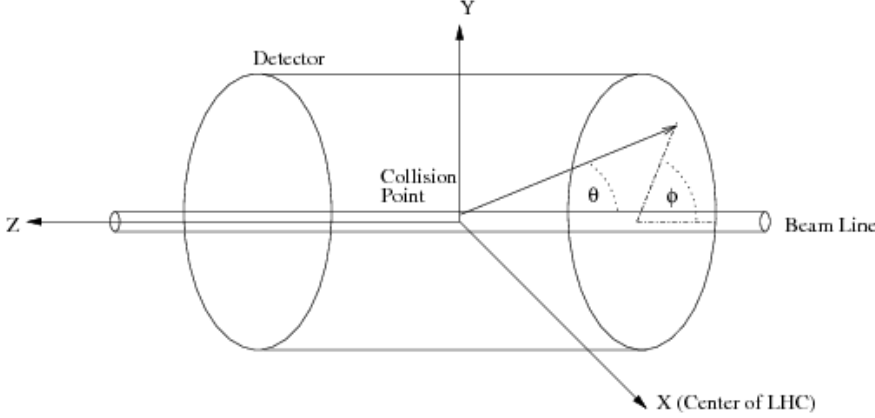


FIGURE 2.5: CMS coordinate system. The x -axis points towards the center of the LHC ring, y -axis points vertically upward, and z -axis points along the beam direction clockwise. Figure from Reference [10].

Polar angle (θ) is the angle measured relative to the z -axis (beam axis) but it is not commonly used because its difference ($\Delta\theta$) is not Lorentz-invariant for pair production events. Thus, **rapidity** (y) [9], a Lorentz-invariant quantity, is used which is defined as:

$$y = \frac{1}{2} \ln \left(\frac{E + cp_z}{E - cp_z} \right) \quad (2.1)$$

For massless particles (particle's mass is negligible when it is traveling near the speed of light which is comparably similar to the events happening inside the collider), rapidity is transformed **pseudorapidity** (η) [9] which is defined as:

$$\eta = -\ln \left[\tan \left(\frac{\theta}{2} \right) \right] \quad (2.2)$$

With this, the **angular separation** between objects is defined as $\Delta R \equiv \sqrt{(\Delta y)^2 + (\Delta\phi)^2}$, or $\Delta R \equiv \sqrt{(\Delta\eta)^2 + (\Delta\phi)^2}$ if particles involved are massless. In addition, the **transverse momentum** (p_T) is defined as the momentum computed from the x and y components, which is transverse to the beam axis, and the **transverse energy** (E_T) is defined as $E_T = E \sin\theta$ [7, 10].

2.2.2 Magnet System

The 13 m long, 6 m inner-diameter, 3.8 T superconducting solenoid of the CMS weighs 220 t cold mass and can provide an enormous bending power of 12 Tm before the muon system measures the muon bending angle. It has a 2.6 GJ stored energy at full current. To support its generation of 3.8 T field (by providing 41.7 MA-turn), the winding is composed of 4 layers, instead of the usual 1 or 2 layers, that is made from an augmented Niobium Titanium (NbTi) conductor [7]. A detailed description of the CMS magnet's parameter is on Table 2.1.

Its main objective is to bend the particles' direction coming from the high-energy collision inside the LHC. The particle's direction is less bent by the magnetic field when it has higher momentum. This anticorrelation between the particle's momentum and bending expresses that its momentum can be measured by tracking its direction. Thus, CMS built the most powerful magnet possible to have a highly accurate measurement of particles' momentum, as well as particles in high energies [11].

The magnetic flux is returned within the detector by the 10,000 t steel **yoke**. It is composed of 2 endcaps, having three disks each, and 5 barrel wheels that weigh from 400 t for the lightest to 1920 t for the central wheel, including the coil and its cryostat. It also acts as a filter that only allows muons and weakly interacting particles (e.g. neutrinos) to pass through [7, 11].

2.2.3 Inner Tracking System

Following the requirements of the LHC physics program, the inner tracking system of the CMS is capable of providing an accurate and efficient reconstruction of the paths of charged particles with $p_T > 1$ GeV within $|\eta| < 2.5$ range. It can also give an accurate measurement of secondary vertices and impact parameters that are essential for effective heavy flavors identification. Its dimension is

TABLE 2.1: Parameters of the CMS magnet.

General Parameters	
Magnetic Length	12.5 m
Cold bore diameter	6.3 m
Central magnetic induction	4 T
Total Ampere-turns	41.7 MA-turns
Nominal current	19.14 kA
Inductance	14.2 H
Stored Energy	2.6 GJ
Cold mass	
Layout	Five modules mechanically and electrically coupled
Radial thickness of cold mass	312 mm
Radiation thickness of cold mass	$3.9 X_0$
Weight of cold mass	220 t
Maximum induction on conductor	4.6 T
Temperature margin wrt operating temperature	1.8 K
Stored energy/unit cold mass	11.6 kJ/kg
Iron yoke	
Outer diameter of the iron flats	14 m
Length of barrel	13 m
Thickness of the iron layers in barrel	300, 630, and 630 mm
Mass of iron in barrel	6000 t
Thickness of iron disks in endcaps	250, 600, and 600 mm
Mass of iron in each endcap	2000 t
Total mass of iron in return yoke	10,000 t

5.8 m long and 2.5 m in diameter enclosing the intersection point. The silicon-based design is due to requiring the system to have high granularity and quick response in a way that the paths are identified consistently and the bunch crossing are attributed precisely without overheating the system and causing severe radiation damage by the intense particle flux [7].

There are two kinds of tracker subsystem in the CMS tracker; a **pixel detector** and a **strip tracker**. The pixel detector has three barrel layers occupying a radial distance from 4.4 to 10.2 cm while the strip tracker has ten barrel detection layers with a radial coverage from 25.5 to 108 cm. Both subsystems are finished off by

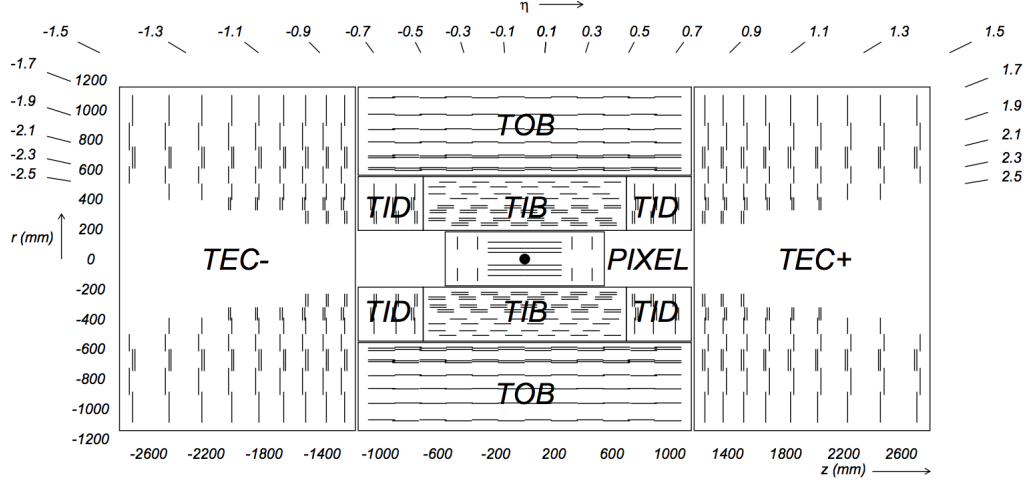


FIGURE 2.6: Schematic cross section view of the CMS tracker system. Each line represents a detector module, double lines means back-to-back module. Figure from Reference [7].

an endcap; two disks for pixel detector and 3 plus 9 disks for strip tracker on each barrel's side. This extends the tracker's acceptance up to $|\eta| < 2.5$. Overall, the CMS tracker is composed of 1440 pixel and 15,418 strip detector modules. The active silicon area of the CMS tracker is about 200 m^2 [7].

Pixel Detector

Being the closest to the interaction region, the pixel subsystem provides precise tracking points in the transverse ($r - \phi$) and longitudinal (z) plane; thus it is responsible for the small impact parameter resolution for accurate reconstruction of secondary vertices from b and τ decays, and formation of seed tracks for the outer track reconstruction and high-level triggering. It covers a range of $|\eta| < 2.5$ to match the acceptance of the central tracker [7].

The dimension of the pixel cell is $100 \times 150 \mu\text{m}^2$. It uses a concept called “n-in-n” where the pixels contain n-implants placed in the n-substrate while the back side is p-doped. This concept was chosen, compare the usual single sided “p-in-n”, because: (1) a high signal charge is guaranteed at moderated bias voltages (< 600 V) after high hadron fluences, (2) the electrons have high mobility in which the Lorentz angle increases thus satisfying the spatial resolution requirement,

and (3) the necessity of constructing the back leads to the implementation of the guard ring system which keeps all sensor edges at ground potential [12].

The 53 cm long three barrel layers (BPix) contain 48 million pixels with a total area of 0.78 m^2 while the two 6-15 cm radius endcap disks (FPix) contain 18 million pixels covering a total area of 0.28 m^2 [7].

Strip Tracker

The strip tracker subsystem, which encloses the pixel detector subsystem, is built with 24,244 single-sided “p-on-n” type microstrip sensors. A total of 9.3 million strip trackers that covers a total active area of 198 m^2 is used in this subsystem. The sensors are manufactured on 6-inch wafers in a standard planar process having an n-doped float zone silicon with $\langle 100 \rangle$ crystal orientation. There are two sets of sensors made: (1) the “thin” with a $320 \mu\text{m}$ wafer thickness and a $1.5 \div 3.25 \text{ K}\Omega\text{cm}$ substrate resistivity, and (2) the “thick” with a $500 \mu\text{m}$ wafer thickness and a $4 \div 8 \text{ K}\Omega\text{cm}$ requested resistivity [13].

The subsystem can be divided into quarters; the four layers **Tracker Inner Barrel** (TIB), the six layers **Tracker Outer Barrel**, the **Tracker Inner Endcap** (TID) that is made of three small disks of the inner barrel on both side, and the **Tracker Outer Endcap** (TEC) which is composed of nine big disks on both sides of the tracker. The TIB and TID have a combined radius of 55 cm and delivers up to $4 r - \phi$ measurements on a trajectory using “thin” sensors, parallel to the beam axis for TIB and radial for TID. The TOB has a radius of 116 cm and uses “thick” sensors. It provides $6 r - \phi$ measurements per trajectory. Lastly, the TEC covers the region $124 \text{ cm} < |z| < 282 \text{ cm}$ and $22.5 \text{ cm} < |r| < 113.5 \text{ cm}$. It carries up to 7 rings of microstrip sensors (the inner 4 rings use “thin” sensors and the outer 3 rings use “thick” sensors) and delivers $9 r - \phi$ measurements per trajectory [7, 13].

2.2.4 Electromagnetic Calorimeter

The ECAL system is situated right after the inner tracking system. Its objective is to measure the EM particles' energy such as electrons and photons. The main material of the ECAL is the lead tungstate (PbWO_4) crystals; 61,200 mounted in the barrel and 7,324 in both of the endcaps. PbWO_4 crystal is the chosen material for it is highly dense (8.28 g/cm^3), has short radiation length* ($0.89 \text{ cm } X_0$), and small Molière radius[†] ($2.2 \text{ cm } R_M$). The ECAL's high-density crystals design makes it radiation resistive, have a quick temporal response ($\sim 10 \text{ ns}$), and provide fine granularity. Being a homogeneous crystal calorimeter, it also provides a good energy resolution which enhances the search for $H \rightarrow \gamma\gamma$ [7, 14].

The photodetectors used are avalanche photodiodes (APDs) in the barrel and vacuum phototriodes (VPTs) in the endcaps. The **ECAL barrel** (EB) covers a range of $|\eta| < 1.479$ with a granularity of 360-fold in ϕ and (2×85) -fold in η . Its crystals have a front face cross section of $22 \times 22 \text{ mm}^2$ ($0.0174 \times 0.0174 \text{ in } \eta - \phi$), and $26 \times 26 \text{ mm}^2$ at the rear face. The centers of the crystals' front face are at a radius 1.29 m . The crystal has a length of 230 mm ($25.8 \text{ } X_0$). Overall, the barrel crystal's dimension is 8.14 m^3 in volume and 67.4 t in weight. The **ECAL endcap** (EE) covers a range of $1.479 < |\eta| < 3.0$. It is 315.4 cm away from the interaction point longitudinally, considering the estimated 1.6 cm shift towards the interaction point when the magnetic field is turned on. Both endcaps are divided into 2 halves, or *Dees*, with each, holds 3662 crystals. The crystals in the EE are identically shaped and grouped in 5×5 crystals (also known as "supercrystals", or SCs) with a length of 220 mm ($24.7 \text{ } X_0$). It has a front face cross section of $28.62 \times 28.62 \text{ mm}^2$, and $30 \times 30 \text{ mm}^2$ at the rear face. The dimension of the EE crystal is 2.90 m^3 in volume and 24.0 t in weight [7, 14].

*Radiation length X_0 is the distance traveled by the charged particle in a material due to the electromagnetic interaction.

[†]Molière radius R_M is the distance in the transverse plane of an incoming particle that contains $\geq 90\%$ of the shower's energy deposition.

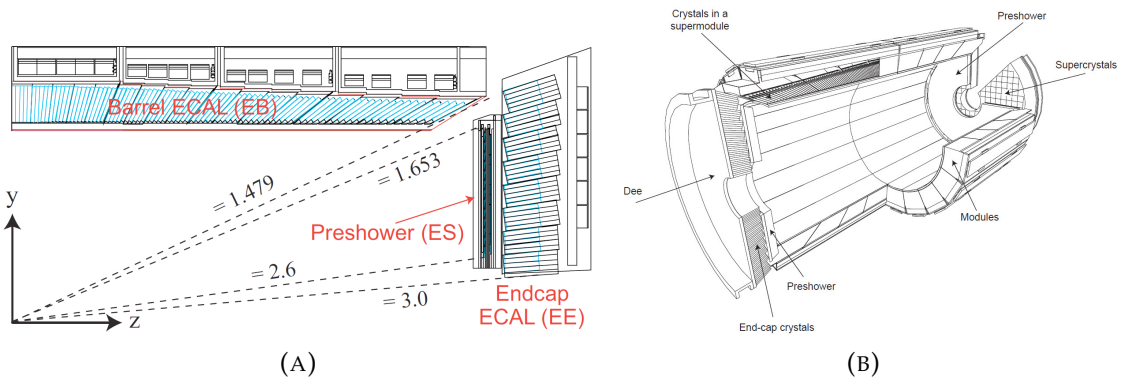


FIGURE 2.7: CMS electromagnetic calorimeter; (A) One-quarter schematic cross section view (dashed lines represent fixed η values) from Reference [15], and (B) Layout of the crystal modules, supermodules, and endcaps, with the preshower in front, in the CMS ECAL from Reference [7].

In front of the EE crystals, there is a **preshower** detector installed within the range of $1.653 < |\eta| < 2.6$. Its objectives are to filter neutral pions (π^0), identifies electrons from minimum ionizing particles, and enhances the electron's and photon's position determination with high granularity. It is made up of silicon strip sensor with a lead absorber, which initiates the electromagnetic showers, in front. Its total thickness is 20 cm [7].

The electromagnetic (EM) energy resolution [7, 14] of the ECAL is defined as:

$$\left(\frac{\sigma}{E}\right)^2 = \left(\frac{S}{\sqrt{E}}\right)^2 + \left(\frac{N}{E}\right)^2 + C^2 \quad (2.3)$$

where S is the stochastic term, which depends on fluctuation in showering, photo-statistics and photodetector gain; N the noise term, which depends on electronic noise level and pile-up; and C is the constant term that depends on leakage of energy, calibration, and non-uniformity of the longitudinal light collection.

2.2.5 Hadron Calorimeter

The HCAL system is placed mainly on the outer extent of the ECAL system ($R = 1.77$ m) and the inner extent of the superconducting solenoid ($R = 2.95$

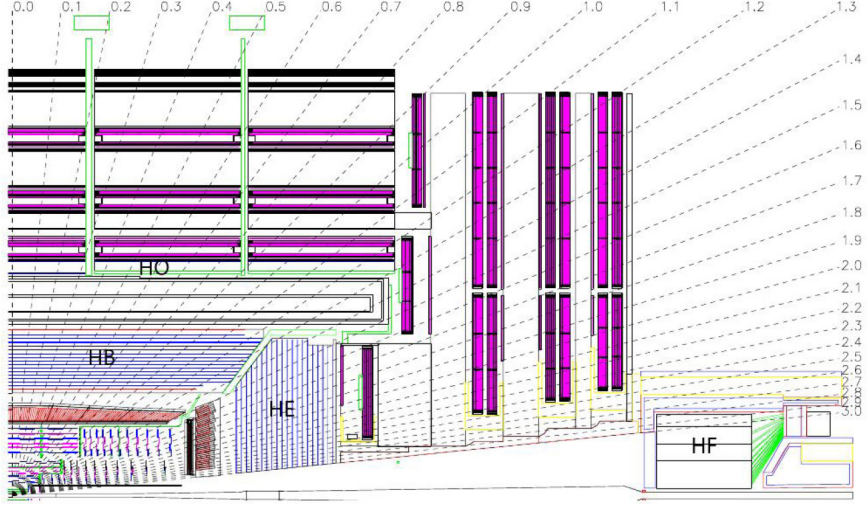


FIGURE 2.8: One-quarter longitudinal view of the CMS hadron calorimeter system showing the layout of its parts: the hadron barrel (HB), endcap (HE), outer (HO), and forward (HF) calorimeter. The dashed lines represent fixed η values.

Figure from Reference [7].

m). It measures the hadron jets and neutrinos or exotic particles that result to the apparent missing transverse energy[‡] (E_T^{miss}). It is divided into four distinct subsystems; the **HCAL barrel** (HB), the **HCAL endcap** (HE), the **HCAL outer** (HO), and the **HCAL forward** (HF) [7, 16].

The HB is placed inside the superconducting solenoid that covers a range of $|\eta| < 1.3$. It consists of 36 azimuthal wedges that divide the barrel into HB+ and HB-. These wedges are made out of flat brass absorber plates which are aligned parallel to the beam axis. The main material used for the absorber is brass, eight layers of 50.5 mm thick plates and six layers of 56.5 mm thick plates, which is in the middle of two steel plate, 40 mm thick in front and 75 mm thick at the back. The total absorber thickness is 5.82 interaction length[§] (λ_l) at 90° . A 3.7 mm thick Kuraray SCSN81 plastic scintillator is used as the active material for the HB [7, 16].

The HE is in within the range of $1.3 < |\eta| < 3$, which is also inside the superconducting solenoid. Same with HB, it also uses brass as the main material

[‡]Missing transverse energy E_T^{miss} is the imbalance in the energy measured in the transverse plane that mainly comes from neutrinos (Neutrinos cannot be detected by the detectors).

[§]Interaction length λ_l is the distance traveled by the hadronic particle through a material due to the nuclear/strong interactions.

for the absorber and scintillator as the active material; 79 mm thick brass disks interleaved with scintillator wedges, 9 mm thick Bicron BC408 for the first layer and 3.7 mm thick SCSN81 for the other layers. Combining HB and HE, the total length of the HCAL system is $\sim 10 \lambda_l$, including the EM crystals [7, 16].

The HO is placed outside the superconducting solenoid that complements the HB. This sequence is due to the constraint in the amount of material that can be put in to absorb the hadronic shower. The HO catches the energy leakage from the HB which $\sim 5\%$ of all hadron's energy above 100 GeV are deposited into it. In ϕ plane, it has a 12-fold structure, with 30° component each that are divided into six 5° sectors. In η plane, it consists of five 19.5 cm thick iron "rings"; Ring 0 covers a range of $|\eta| < 0.35$, Rings ± 1 cover $0.35 < |\eta| < 0.87$ range, and Rings ± 2 cover $0.87 < |\eta| < 1.2$ range. Ring 0 has two layers of HO scintillators on either side at 3.82 m X_0 and 4.07 m X_0 , while the other have single HO scintillator layer at 4.07 m X_0 . The HO extends the depth of the HCAL system to a minimum of $11.8 \lambda_l$ excluding the HB-HE boundary region [7, 16].

Lastly, the HF is situated 11.2 m away from the interaction point that is beyond $|\eta| = 3.0$. The HF extends the pseudorapidity range up to $|\eta| = 5.2$ using a Cherenkov-based, radiation-hard technology. It is made of quartz fiber and steel, with the fibers parallel to the beam axis. It is built in 20° wedges with each contains two $10^\circ \phi$ sectors [7, 16].

The hadronic energy resolution [16] of the HB and ECAL combination can be parameterized as:

$$\frac{\sigma}{E} = \frac{S}{\sqrt{E}} \oplus C \quad (2.4)$$

where S is the stochastic term, and C is the constant term.

2.2.6 Muon Detector

2.3 The Trigger System



Bibliography

- [1] *Experiments*. 2012. URL: <http://cds.cern.ch/record/1997374>.
- [2] *The Large Hadron Collider*. 2014. URL: <http://cds.cern.ch/record/1998498>.
- [3] *Building the HL-LHC with the Industry*. URL: <https://project-hl-lhc-industry.web.cern.ch/>.
- [4] *The accelerator complex*. 2012. URL: <http://cds.cern.ch/record/1997193>.
- [5] Cinzia De Melis. "The CERN accelerator complex. Complexe des accélérateurs du CERN". In: (2016). General Photo. URL: <http://cds.cern.ch/record/2197559>.
- [6] Mike Lamont. "LHC Performance in Run 2 and Beyond". In: *PoS Lepton-Photon2015* (2016), 001. 8 p. URL: <http://cds.cern.ch/record/2257503>.
- [7] CMS Collaboration. "The CMS experiment at the CERN LHC". In: *Journal of Instrumentation* 3.08 (2008), S08004. URL: <http://stacks.iop.org/1748-0221/3/i=08/a=S08004>.
- [8] Tai Sakuma and Thomas McCauley. "Detector and Event Visualization with SketchUp at the CMS Experiment". In: *Journal of Physics: Conference Series* 513.2 (2014), p. 022032. URL: <http://stacks.iop.org/1742-6596/513/i=2/a=022032>.
- [9] Heidi Schellman. *Learn Hardon Collider Physics in 3 Days*. 2005. URL: <http://particle.physics.ucdavis.edu/workshops/TASI04/schellman.pdf>.
- [10] Matthias Schott and Monica Dunford. "Review of single vector boson production in pp collisions at $\sqrt{s} = 7 \text{ TeV}$ ". In: *Eur. Phys. J.* C74 (2014), p. 2916. DOI: [10.1140/epjc/s10052-014-2916-1](https://doi.org/10.1140/epjc/s10052-014-2916-1). arXiv: [1405.1160 \[hep-ex\]](https://arxiv.org/abs/1405.1160).
- [11] *Bending Particles*. URL: <http://cms.cern/detector/bending-particles>.

- [12] Y. Allkofer et al. "Design and performance of the silicon sensors for the CMS barrel pixel detector". In: *Nucl. Instrum. Methods Phys. Res., A* 584.physics/0702092 (2008). Comments: 22 pages, 21 figures, pp. 25–41. URL: <http://cds.cern.ch/record/1142546>.
- [13] Laura Borrello et al. *Sensor Design for the CMS Silicon Strip Tracker*. Tech. rep. CMS-NOTE-2003-020. Geneva: CERN, 2003. URL: <http://cds.cern.ch/record/687861>.
- [14] CMS Collaboration. "Performance and operation of the CMS electromagnetic calorimeter". In: *Journal of Instrumentation* 5.03 (2010), T03010. URL: <http://stacks.iop.org/1748-0221/5/i=03/a=T03010>.
- [15] Bora Isildak. "Measurement of the differential dijet production cross section in proton-proton collisions at $\sqrt{s} = 7$ tev". PhD thesis. Bogazici U., 2011. arXiv: [1308.6064 \[hep-ex\]](https://arxiv.org/abs/1308.6064). URL: <https://inspirehep.net/record/1251416/files/arXiv:1308.6064.pdf>.
- [16] CMS Collaboration. "Performance of the CMS hadron calorimeter with cosmic ray muons and LHC beam data". In: *Journal of Instrumentation* 5.03 (2010), T03012. URL: <http://stacks.iop.org/1748-0221/5/i=03/a=T03012>.

